Evaluation of material degradation of 1Cr-1Mo-0.25V steel by ball indentation and resistivity

CHANG-SUNG SEOK, JAE-MEAN KOO
School of Mechanical Engineering, Sungkyunkwan University, 300 Chunchun-dong, Jangan-gu, Suwon, Kyonggi-do 440-746, Korea

Published online: 4 February 2006

In this study, test materials with several different degradation levels were prepared by isothermal aging heat treatment at 630 °C up to 1820 h. Tensile and fracture tests were performed and those were compared with BI tests and DC potential drop method. These results show that normalized Brinell hardness agrees well with normalized tensile strength at the viewpoint of material degradation and the tensile strength and fracture toughness of degraded material can be determined by Brinell hardness or resistivity.

1. Introduction

Material degradation is usually observed in deterioration of mechanical properties due to the changes in microstructure of materials on long-terms exposure at high temperatures. Because this degradation of mechanical properties is an important factor that affects the safe operation of facilities, it's required to estimate the extent of degradation [1–3]. But since it is difficult to take specimens from the operating components to evaluate mechanical properties of components, non-destructive techniques are needed to estimate the degradation.

The BI (Ball Indentation) tests [4] have the potential to assess the mechanical and fracture properties non-destructively and to replace conventional fracture tests. These tests were shown to yield $\sigma-\varepsilon$ curves that correlated well with the standard destructive tensile tests.

One of non-destructive methods widely used is DC potential drop method which has a strong point in view of applicability to in-service facilities. In particular, it is known that the resistivity is sensitive to not only the variation of macroscopic structure but also that of the micro-structure due to material degradation. The four-point probe has proven to be a convenient method for measuring resistivity [5].

In this study, test materials with several different degradation levels were prepared by isothermal aging heat treatment at 630°C up to 1820 h. The effects of aging on the mechanical properties of each specimen were investigated by tensile test and fracture toughness test. Then those were compared with BI tests and DC potential drop method. These results show that these methods are useful to estimate the extent of degradation. In particular, it has been seen that normalized Brinell hardness agrees well with normalized tensile strength at the viewpoint of material degradation and tensile strength and fracture toughness of degraded material can be determined by Brinell hardness or resistivity.

2. Fracture toughness test, ball indentation method, and DC potential drop method

2.1. Fracture toughness test

Fracture toughness test by the ASTM E399-90 [6] is to find the lower limiting value of the plane-strain fracture toughness, and the overall dimensions of the compact tension (CT) specimen for various measurement capacities are specified by the standards. The length of the crack, a, consists of two elements. One is the notch (with a taper section) and the other is a sharp length of precracking created by cyclic loading and unloading of the specimen.

The specimen dimensions must be sufficiently large in comparison with the plastic zone dimensions. The three relevant dimensions are crack length, a, specimen thickness, B, and uncracked ligament length, w-a, the following size requirements are normally specified:

$$a, B > 2.5\left(\frac{K_{\mathrm{Ic}}}{S_y}\right)^2 \tag{1}$$

where K_{Ic} is the fracture toughness and S_{y} denotes the yield strength.

0022-2461 © *2006 Springer Science + Business Media, Inc.*
DOI: 10.1007/s10853-005-3644-6

If the clip gauge is placed at the mouth of the notch, the cracking opening can be measured and the corresponding load can be recorded to develop a load displacement curve with a straight line portion. The usual testing procedure is to increase the tensile load, P, until fast fracture is initiated, as indicated by a gross non-linearity in the load-displacement record. Theprocedure by which the exact load at fast fracture, P_Q, is determined is clearly explained in the standards.

Finally, the stress intensity factor at failure, K_Q, may be determined via the following equation,

$$K_I = \frac{P}{B(w)^{1/2}}\left[29.6\left(\frac{a}{w}\right)^{0.5} - 185.5\left(\frac{a}{w}\right)^{1.5} + 655.7\left(\frac{a}{w}\right)^{2.5} - 1017\left(\frac{a}{w}\right)^{3.5} + 639\left(\frac{a}{w}\right)^{4.5}\right] \quad (2)$$

where w is the width of plate. If the size criteria of Equation 1 are satisfied, K_Q may be accepted as a valid plane strain fracture toughness.

2.2. Ball indentation method

The Ball indentation (BI) test is based on strain-controlled multiple indentations of a polished surface by a spherical indenter at a single penetration location. The indentation loads and penetration depths are measured during the test, and are used to calculate the stress-strain values from elasticity and plasticity theories and semi-empirical relationships which govern the behavior of material under multiaxial indentation loading. By analyzing the stress-strain curve, tensile parameters of material such as yield strength, tensile strength, strength coefficient, and strain hardening exponent as well as fracture toughness can be evaluated [7]. Mathew and Murty [8] studied on tensile and fracture properties of molybdenum using the ball indentation technique. Tests have been carried out at several temperatures in the range of 148 to 423 K at a constant strain rate. They reported that tensile properties determined from these tests agreed well with published results from conventional tensile tests.

Using the Hertzian equation the plastic depth h_p, is converted into plastic indentation diameter d_p (Fig. 1),

$$d_p = \sqrt[3]{\frac{0.5C\,D\left[h_p^2 + (d_p/2)^2\right]}{\left[h_p^2 + (d_p/2)^2 - h_p D\right]}} \quad (3)$$

where D is the indenter diameter and C=5.47P(1/E_1+1/E_2). P is the load and E_1 and E_2 are the elastic moduli of indenter and specimen respectively. True plastic strain ε_p can be obtained from the following equation.

$$\varepsilon_p = 0.2d_p/D \quad (4)$$

The true plastic stress σ can be calculated from the Hertz theory for normal contact between elastic solids,

$$\sigma = 4P/\pi d_p^2\delta \quad (5)$$

where δ is a constraint factor that depends on the material parameters such as strain-rate sensitivity. The stress is smaller than the mean indentation pressure because the plastic deformation of the materials is constrained by the surrounding elastic material. The true stress versus true strain curve can be represented by the power law equation.

$$s = K\varepsilon_p^n \quad (6)$$

where n is the strain hardening exponent and K is the strength coefficient (provided the plot of the data ln σ versus ln ε_p is linear). Values of K and n are determined by linear regression analysis of the data. For $\varepsilon_p = n$ [8], Equation 6 will provide the expression for true ultimate tensile strength. The engineering value of ultimate tensile strength can be obtained from the following equation.

$$S_{UTS} = K\left(\frac{n}{e}\right)^n \quad (7)$$

where $e = 2.71$.

Yield strength is estimated from the relationship between the mean pressure and impression diameter as developed by Meyer [4]. Data points from all loading cycles (maximum value of $d_t/D = 1.0$) are fit by linear regression analysis to the following relationship:

$$\frac{P}{d_t^2} = A\left(\frac{d_t}{D}\right)^{m-2} \quad (8)$$

where d_t is the total diameter of the impression and m is the Meyer's exponent (m generally has a value between 2 and 2.5) and A is a material yield parameter obtained from the regression analysis. The value of d_t is determined from total depth of penetration (Fig. 1) using the following equation.

$$d_t = 2\sqrt{Dh_t - h_t^2} \quad (9)$$

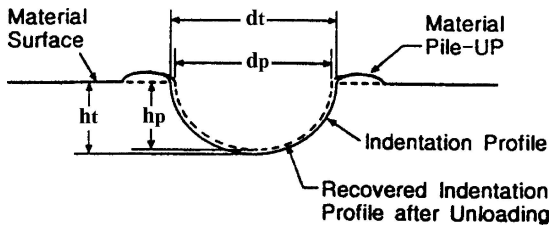

Figure 1 Schematic diagram of a ball indentation profile.

where h_t is the total depth of the indentation. The yield strength (σ_y) is proportional to the Meyer hardness ($4P/\pi d^2$). d is the final impression diameter and can be calculated using the following equation.

$$\sigma_y = \beta_m A \tag{10}$$

Here β_m and A are constants for a given materials. The value of β_m is determined from yield strength obtained from standard tensile tests.

2.3. DC potential drop method

In this study, resistivity was gotten on the basis of "Standard Test Method for Measuring Resistivity of Silicon Wafers with an In-Line Four-Point Probe (ASTM F84-93, 1993)". The potential, V is given at the distance r from the electrode, when the current I flows through the electrode:

$$V = \frac{\rho I}{2\pi r} \tag{11}$$

where ρ is resistivity. The basic model for four point probe measurement is shown in Fig. 2. Four probes are placed on a flat surface of the material to be measured. Current is passed through the two outer probes, and the potential is measured across the inner pair [9, 10]. Based on the relative magnitudes of the specimen thickness (t) and the probe spacing(s), the resistivity is computed as follows.

$$\rho = 2\pi s\left(\frac{V}{I}\right), \quad \text{for } t \gg s \tag{12}$$

and

$$\rho = \frac{\pi t}{\ln 2}\left(\frac{V}{I}\right), \quad \text{for } t \ll s. \tag{13}$$

Equations (12) and (13) are derived from the presumptions for thick and thin specimen respectively, but the real specimen is different. Since an error for resistivity is actually occurred at measurement by dimensional constraints, a correction factor k is used to take into account the shape of the specimen and probe.

$$\rho_s = k\left(\frac{V}{I}\right). \tag{14}$$

The correction factor k consists with the correction factor F for corresponding thickness of specimen (t/s) and correction factor C for corresponding width of specimen (d/s, a/d) to consider the shape of specimen and probe. F and C are found from referring to Smits' table [5]. The probes, which take maintenance over the distance 4 s from each edge of the boundaries of the specimen, must be placed at the center of the specimen surface [11, 12].

Masahiko Ikeda et al. [13] compared tensile strength with Vickers hardness(HV) of Ti-15Mo-5Zr-3Al alloy with isothermal aging at 673 and 773 K, and reported that the increment in HV is roughly proportional to decrement in resistivity ratio. Also, since it was reported that tensile strength increases almost linearly with the increase in HV, they indirectly verified the relationship between resistivity and tensile strength.

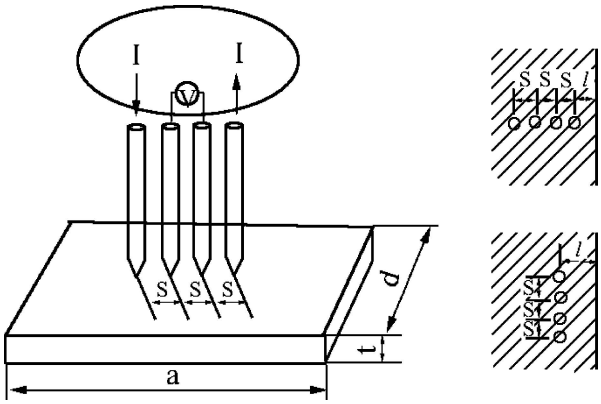

Figure 2 Configuration of specimen boundary and 4 point probe.

3. Experiment

3.1. Aging materials

Low-alloy ferritic steel, 1Cr-1Mo-0.25V, is widely used as high temperature structural components in electric power generation industries. The chemical composition of materials is given in Table I. In this study, the aging materials were prepared to simulate the field conditions by accelerated aging method. The temperature of aging was selected to be 630°C that is higher than that under the operating conditions of around 538°C.

Aging times were determined by the diffusion theory of Fe at the operating (538°C) and aging temperatures (630°C) [14, 15],

$$t_2 = t_1 \exp\left[\frac{Q}{R}\left(\frac{1}{T_2} - \frac{1}{T_1}\right)\right] \tag{15}$$

where R is the gas constant t (8.314 J/kmol/K) and Q is the activation energy (65 kcal/mol) for the self diffusion of Fe and T_1, T_2 are operating and aging temperatures, t_1 and t_2 are the corresponding aging times at T_1 and T_2. The obtained aging time at 630°C for equivalent microstructure at 538°C are given in Table II.

Microstructure of the virgin and degraded materials was characterized using an optical microscope. Accord-

TABLE I Chemical composition of 1Cr-1Mo-0.25 V (Wt.%)

C	Si	Mn	S	P	Ni	Cr	Mo	V	Sn
0.29	0.01	0.74	0.004	0.007	0.060	1.29	1.24	0.25	0.0047

TABLE II Aging time at 630°C for equivalent micro-structure serviced at 538°C

Aging time at 538°C (hour)	0	25,000	50,000	100,000
Aging time at 630°C (hour)	0	453	933	1,820

TABLE III Results of tensile tests and fracture toughness tests

Aging time (hour)	Yield strength (0.2% offset) (MPa)	Tensile strength (MPa)	K_Q (Nmm$^{-3/2}$)
0	711	844	3,863
453	533	676	3,304
933	481	615	2,761
1,820	450	582	1,771

ing to ASTM E8-95, tensile tests were performed using a universal test machine at room temperature. The fracture toughness (K_{IC}) test was carried out using a 25 ton hydraulic dynamic tester (Instron Model 1332) according to ASTM E 399-90. CT typed specimens in 25.4 mm thick were used. The test was conducted with an A/D converter and a PC to control the test and analyze data. First, P_Q was determined according to ASTM E 399 and then, K_Q was determined. But because the tests didn't satisfy the size requirements for a valid K_{IC}, $B \geq 2.5(K_Q/\sigma_{ys})^2$, the results of toughness tests were transcribed as K_Q (Table III).

3.2. BI and DC potential drop method experiment

Ball indentation tests were performed on materials degraded at the laboratory. A tungsten carbide spherical indenter of 0.508 mm diameter was used for the BI tests. The tests were carried out with an indenter velocity of 0.005 mm/s at room temperature. The loading-unloading process was carried out in seven steps.

The instrument for measuring resistivity consists of the four probes, the current meter, the voltage meter and Whiston bridge, which can control the direction of the current. The distance between the probes was 1.59 mm.

When measuring for resistivity, it requires that the proper current be supplied because heating at the contact points causes a fluctuation of measurement. In this experiment, the current of 1A was supplied for the specimen and the experimental temperature was maintained at 13.5°C in the insulation box to eliminate the effect of the external temperature. After getting a stable condition for measuring resistivity, and then the voltage meter and the current meter were fixed on the reference voltage and the reference current set to zero. Data were obtained with 3 to 4 measurements for each specimen after appropriate corrections for electrode thermoelectromotive force caused by the thermal effect at the contact points. The error in the resistivity was estimated to be less than 0.2% while it is around 0.1% in majority of the cases.

4. Result and correlations

The results from the non-destructive methods, that is, BI and resistivity, are now correlated with the mechanical properties measured using standard tensile and fracture tests.

Fig. 3 shows the microstructure of the material for each degradation time. Coarsening of carbides is noted along with precipitation at the grain boundaries with aging time. These changes of microstructure are expected to decrease in strength with increasing aging time.

Fig. 4 shows the effect of aging time on $\sigma-\varepsilon$ curves from tensile testing results. We note that strength decreased and ductility increased with aging time.

The true stress vs. strain curves derived from BI tests are included in Fig. 5 for the virgin and aged materials and we note strength decreased with aging as was observed in the standard tensile tests (Fig. 4).

Fig. 6 shows the effect of degradation time on electrical resistivity. We can note that the electrical resistivity decreased with increasing aging time.

Fig. 7 shows the effect of aging time on normalized factors, i.e., Brinell hardness, yield strength, and tensile strength of tensile and BI tests at in-service temperature, 538°C, respectively. Normalized factors are the values of aged materials divided by those of virgin. This result shows that normalized Brinell hardness has a little deviation from normalized yield strength by tensile test but agrees well with others. Hence, it can be seen that the effect of degradation time on tensile strength can be estimated by Brinell hardness.

Fig. 8 shows the effect of degradation time on normalized factors, i.e., yield strength, Brinell hardness, fracture toughness, and electrical resistivity at in-service temperature, 538°C. Normalized Brinell hardness and yield strength were similarly decreased with respect to degradation time and electrical resistivity was decreased slightly. While Tensile strength, yield strength and electrical resistivity are not linearly related, fracture toughness is linearly related with degradation time. Hence fracture toughness is a useful factor for evaluating the degree of material degradation. That is,

$$\frac{K_Q}{K_{Q0}} = A_d t + 1 \tag{16}$$

where t is the degradation time and K_{Q0} are fracture toughness of virgin material and $A_d = -5\times10^{-6}$.

The decrease of the fracture toughness can be interpreted as the weakness of material due to intergranular brittleness as degraded.

Fig. 9 shows the exponential relation between normalized fracture toughness and normalized Brinell hardness.

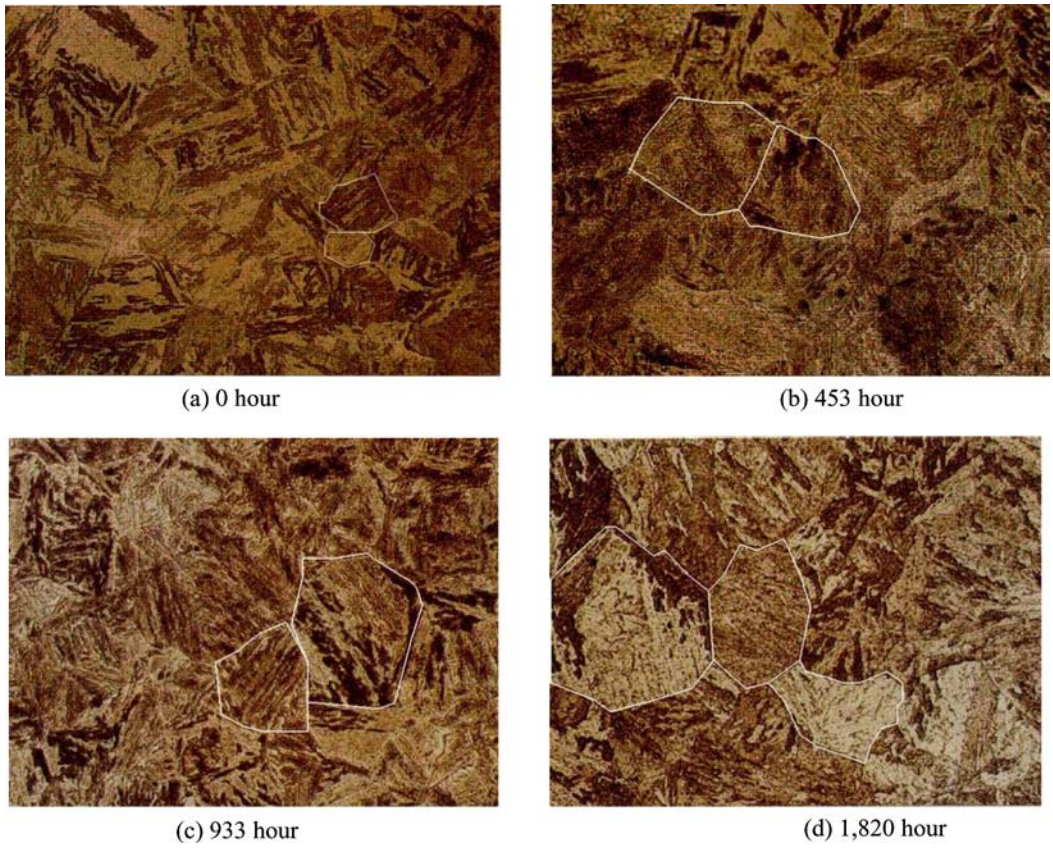

Figure 3 Microstructure (×400) for each material after aging for (a) 0 h (b) 453 h (c) 933 h and (d) 1820 h at 630°C.

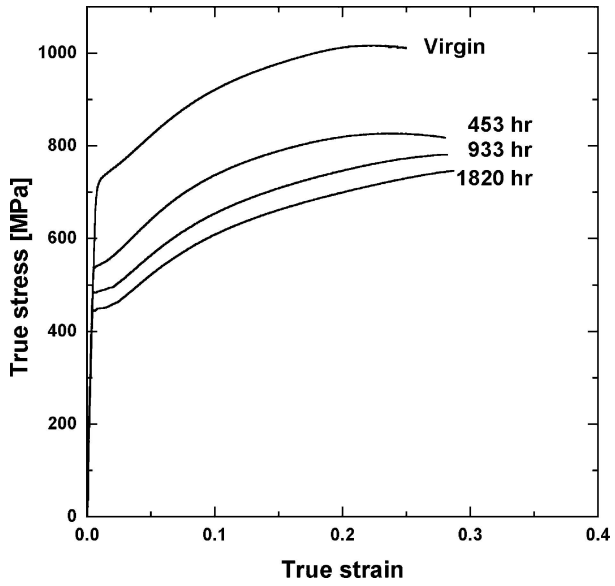

Figure 4 Effect of aging time on $\sigma - \varepsilon$ curves.

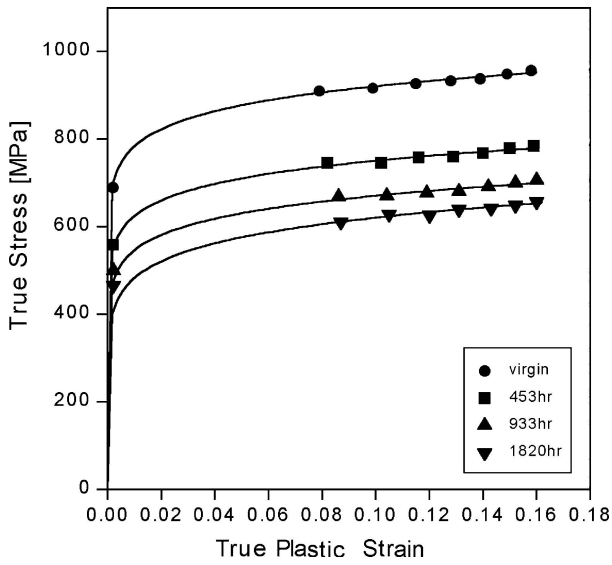

Figure 5 True stress-strain curves derived from BI tests.

That is,

$$\frac{K_Q}{K_{Q0}} = D_d - E_d e^{-F_d z} \tag{17}$$

where $z = \frac{HB}{HB_0}$ and D_d=1.048 and E_d=129.435 and F_d=8.097. If normalized Brinell hardness can be obtained by BI test, normalized fracture toughness can be determined by Equation (17) and it means that also the degree of material degradation can be determined by BI test.

The BI test is a quasi-nondestructive method to get material properties without the destruction of the material. This method has the strong points of being applicable to in-service facilities and being able to get reliable data without the influence of an experimentalist's skill and so

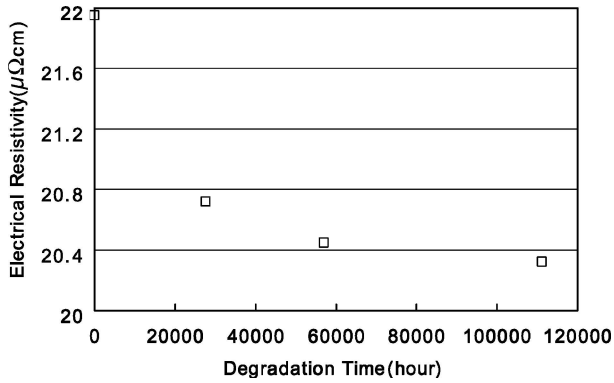

Figure 6 Effect of degradation time on resistivity.

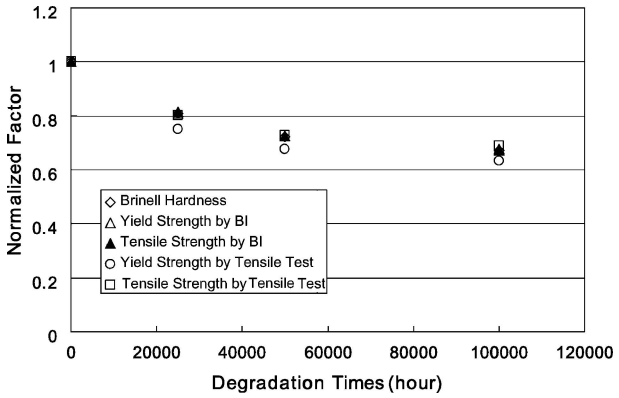

Figure 7 Effect of degradation time on normalized factors by BI and tensile tests.

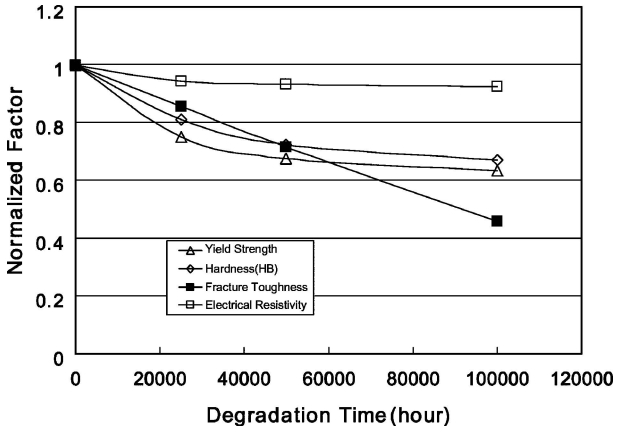

Figure 8 Effect of degradation time on normalized factors.

on. It is expected to be able to estimate not only general mechanical properties like tensile strength and hardness but also fracture properties like fracture toughness at the viewpoint of material degradation.

Fig. 10 shows the relation of normalized tensile strength and normalized resistivity. There is the linear interrelation between them as follow.

$$\frac{\sigma_{TS}}{\sigma_{TS0}} = B_d \frac{\rho}{\rho_0} - C_d \qquad (18)$$

where σ_{TS0} are tensile strength of virgin material and B_d=4.038 and C_d=3.033 and ρ/ρ_0 is normalized resistivity, the rate of aged resistivity (ρ) divided by the reference resistivity (ρ_0). By using Equation 18, tensile strength of degraded material of 1Cr-1Mo-0.25V can be obtained from resistivity at in-service temperature, 538°C.

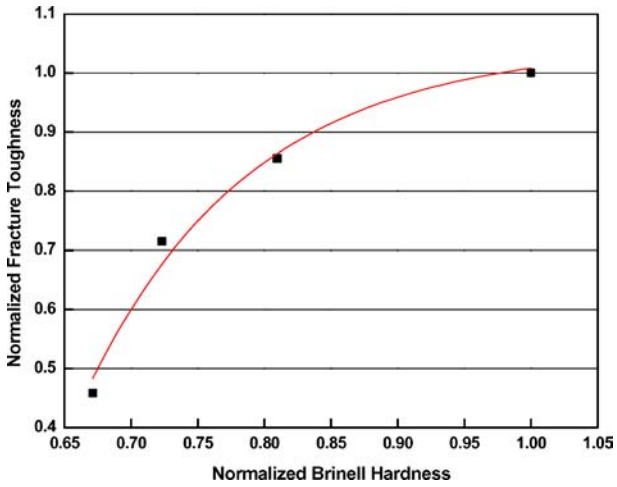

Figure 9 Relation between normalized Brinell hardness and normalized fracture toughness at service temperature.

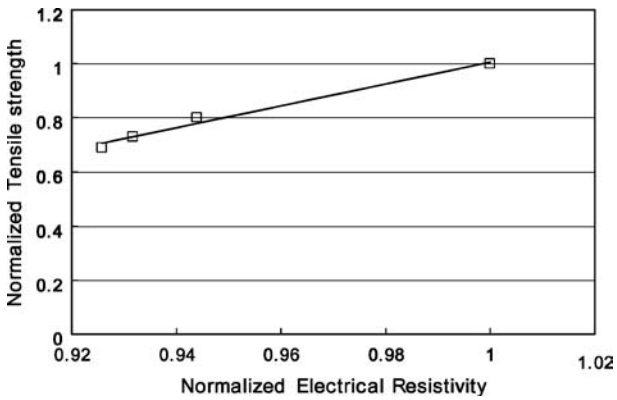

Figure 10 Relation between normalized tensile strength and normalized electrical resistivity.

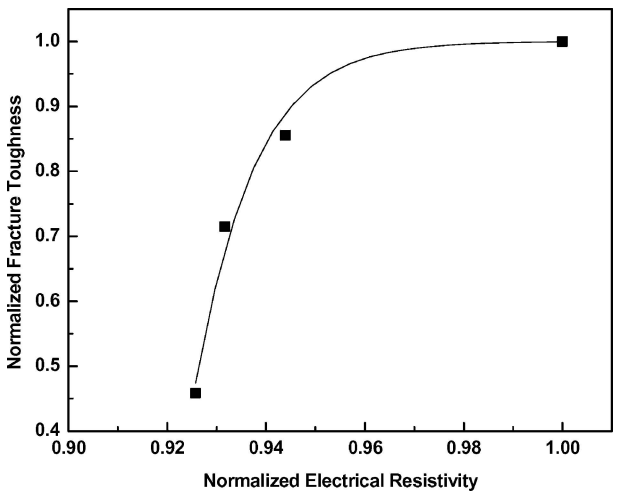

Figure 11 Relation between normalized fracture toughness and normalized electrical resistivity.

Fig. 11 shows the relation of normalized fracture toughness and normalized resistivity. There is the interrelation

between them as follow.

$$\frac{K_Q}{K_{Q0}} = \frac{A_1 - A_2}{1 + e^{(x-x_0)/dx}} + A_2 \tag{19}$$

where $x=\rho/\rho_0$ and $x_0=0.903$ and $A_1=-3.748$ and $A_2=1$ and $dx=0.011$. Fracture toughness can be calculated from resistivity by using Equation 19 in the same condition. Hence, we can see that it is possible to evaluate material degradation using DC potential drop method.

5. Conclusion

In this study, the effect of aging on the mechanical behavior of 1Cr-1Mo-0.25V steels has been studied using tensile test, fracture toughness test, ball indentation test and DC potential drop method. Since the results are about the aged materials of 1Cr-1Mo-0.25V steels, those have a limit but are summarized as follows:

(1) Normalized Brinell hardness agrees well with normalized tensile strength at the viewpoint of material degradation.

(2) Because fracture toughness is linearly related with in-service degradation time, fracture toughness is a useful factor for evaluating the degree of material degradation.

(3) The tensile strength and fracture toughness of degraded material can be determined by Brinell hardness or electrical resistivity.

Acknowledgement

The authors are grateful for the support provided by a grant from Safety and Structural Integrity Research Centre at Sungkyunkwan University and the Brain Korea 21 Project in 2003.

References

1. R. VISWANATHAN and S. GEHL, *idid.* **113** (1991) 263.
2. R. VISWANATHAN and S. M. BRUEMMER, *J. Eng. Mater. and Tech. (Transactions of the ASME)* **107** (1985) 316.
3. S. H. NHAM and A. K. KIM, *Trans. the Korea Soc. Mech. Eng. A* **22** (1998) 814.
4. F. M. HAGGAG and R. K. NANSTAD, *The Amer. Soc. of Mech. Eng. PVP*. **170** (1989) 41.
5. F. M. SMITS, *The Bell Sys. Tech. J.* **37** (1958), 711.
6. ASTM E 399-90, in Annual Book of ASTM Standard (1995), p. 412.
7. F. M. HAGGAG and K. L. MURTY, in "Non-destructive Evaluation and Materials Properties III," edited by P. K. Liaw *et al*., (Warrendale PA, TMS, 1997), p. 101.
8. M. D. MATHEW and K. L. MURTY, *J. Mater. Sci.* **33** (1999) 1497.
9. ASTM B193-87, in Annual Book of ASTM Standard (1992) p. 308.
10. ASTM F84-93, in Annual Book of ASTM Standard (1993) p. 135.
11. J. SHI and Y. SUN, *Rev. Sci. Ins.* **68** (1997) 1814.
12. M. YAMASHITA, T. NISHII and H. KURIHARA, *Jap. J. Appl. Phy.* **35** (1996) 1948.
13. M. IKEDA, S.-Y. KOMATSU, T. SUGIMOTO and M. HASEGAWA, *Mater. Sci. and Eng. A* **243** (1998) 140.
14. A. M. ABDEL-LATIF, S. M. CORBETT and D. M. R. TAPLIN, *Metal Sci.* **16** (1982) 90.
15. A. M. ABDEL-LATIF, J. M. CORBETT, D. SIDEY and D. M. R. TAPLIN, in "*Advanced in Fracture Research,*" Proc. of 5th Int. Conf. on Fracture (ICF5)), 4 (1981) p. 1613.

Received 2 March 2004
and accepted 22 June 2005